

Characteristics of curcumin-loaded poly (lactic acid) nanofibers for wound healing

Thuy Thi Thu Nguyen · Chiranjit Ghosh ·
Seong-Gu Hwang · Lam Dai Tran ·
Jun Seo Park

Received: 5 April 2013 / Accepted: 11 June 2013 / Published online: 25 June 2013
© Springer Science+Business Media New York 2013

Abstract Curcumin (Cur) is a well-known extract of the root of *Curcuma longa* L. that has multi biological functions such as anti-oxidation, anti-inflammatory, anti-cancer, and wound healing properties. In the present study, poly (lactic acid) (PLA) nanofibers were used as a carrier for Cur because PLA nanofibers are biocompatible and have a high-specific surface area and high porosity, which can enhance the functional properties of Cur. The chemical and biological characteristics of Cur/PLA blended nanofibers containing varied amounts of Cur were examined. An increase from 0.125 to 6.250 wt% Cur in PLA caused a decrease in the diameters of the nanofibers from 971 ± 274 to 562 ± 177 nm. At Cur concentrations of <1.250 wt%, PLA and Cur showed good miscibility in the blended nanofibers, as shown by FTIR analysis and tensile tests. The inclusion of Cur in the blended nanofibers at concentration as low as 0.125 wt% promotes the attachment and proliferation of cells. The in vivo wound healing capability of Cur-loaded PLA nanofibers was assessed in a mouse model; treatment with Cur-loaded PLA nanofibers significantly increased the rate of wound closure (87 %) by day 7 compared with that of PLA nanofibers (58 %). The

results of this study suggest that Cur-loaded nanofibers with appropriate Cur concentration are nontoxic and have potential as component of wound-healing patches.

Introduction

Nanofibers, which are fabricated by electrospinning, have attracted significant attention over the last two decades owing to their extremely high-specific surface area and porosity and excellent pore interconnectivity [1, 2]. These characteristics are particularly attractive for biomedical applications. For example, nanofiber scaffolds closely mimic the natural extra cellular matrix structure that supports cell attachment and proliferation; therefore, nanofibers are excellent candidates for tissue engineering and functional wound-dressing materials [3, 4]. Nanofibers-based wound-dressing materials have several advantages over conventional wound dressing such as gauzes, hydrogels, foams, and sponges [5]. Structured nanofiber scaffolds with small pore and a high surface area to volume ratio can promote hemostasis without the use of a hemostatic agent, maintain an appropriately moist environment for the wound by facilitating oxygen permeation and allowing fluid accumulation, effectively protect the wound from bacterial penetration, and be easily functionalized with therapeutic compounds. Consequently, nanofibers are promising materials for facilitating wound healing and skin regeneration. A variety of materials including collagen, gelatin, fibrinogen, chitosan, poly (urethane), poly (caprolactone), poly (lactic acid) (PLA), and some blends of these materials have been electrospun and evaluated for wound healing and dermal reconstitution [6–9]. It has been reported that nanofibrous mats composed of collagen induce cell migration and proliferation, and display

T. T. T. Nguyen · J. S. Park (✉)
Division of Chemical Engineering, Hankyong National
University, 327 Chungang-ro, Gyeonggi-do,
Anseong-si 456-749, Korea
e-mail: jspark@hknu.ac.kr

C. Ghosh · S.-G. Hwang
Department of Animal Life and Environmental Science,
Hankyong National University, 327 Chungang-ro, Gyeonggi-do,
Anseong-si 456-749, Korea

L. D. Tran
Institute of Materials Science, Vietnam Academy of Science
and Technology, Hanoi, Vietnam

effective wound-healing performance with an active response to human fibroblasts in the early state [10, 11]. The main characteristics of nanofiber mats that influence wound-healing performance are their porosity, air permeability, and surface wettability [12]. Additionally, functional compounds including antibiotic agents, growth factors, and even cells can be integrated into nanofiber mats to promote wound healing [5, 8, 13, 14]. According to a study by Schneider et al. [13], a silk nanofiber scaffold electrospun with epidermal growth factor increased the wound closure by 90 % in an in vivo test on mice.

Curcumin (1,7-bis(4-hydroxy-3-methoxyphenyl)-1,6-heptadiene-3,5-dione) is a well-known extract from the root of *Curcuma longa* L. [15]. It has been used for centuries as an ingredient in food, cosmetics, and traditional medicine for wound treatment and stomach issues. Extensive studies on the functional properties of curcumin have clearly shown the dose-dependent biological and pharmacological efficacy of curcumin [16]. Cur exhibits strong antioxidant, anti-inflammatory, anti-tumor, and anti-cancer properties, which make it a valuable agent for treating wounds, burns, and a variety of diseases including diabetes, Alzheimer's, and hepatic disorders [17–19]. The effect of the antioxidant properties of Cur on accelerating the wound healing is evidenced by a significant increase in the activities of superoxide dismutase and glutathione peroxidase and decrease in the activity of lipid peroxide [20]. Moreover, re-epithelialization of the epidermis and increased migration of various cells including myofibroblasts, fibroblasts, and macrophages in the wound bed were reported by Sidhu et al. [21]. Extensive neovascularization and increased collagen deposition in the Cur-treated wounds were observed. The results also demonstrated the ability of Cur to enhance the rate of wound closure in vivo in rats and guinea pigs.

Due to its poor solubility in water, it is difficult to achieve high bioavailability of Cur in the body through oral administration [22]. Additionally, when administered orally, Cur is excreted in the urine and feces [23]. Therefore, the development of appropriate and effective methods for delivering Cur with improved in vivo stability and bioavailability has been a recent focus. Intravenous formulations of Cur have been developed and involve by encapsulating Cur into biodegradable poly (ethylene glycol)-poly (caprolactone) micelles [22], oil-in-water emulsions [23], and chitosan and bovine serum albumin microspheres [24]. Cur has also been incorporated into collagen films [25], β -chitin sheets [26], and polymer nanofibers [27, 28] to fabricate highly effective wound-healing patches. These studies provide firm evidence that the Cur incorporated in these substrates maintains its biological activity and is effective at accelerating dermal wound healing.

In this study, Cur-loaded PLA nanofiber mats were fabricated for the purpose of developing a functional wound dressing. PLA was selected as the supporting material because it is biodegradable, biocompatible, and can support the proliferation and attachment of various cells [29, 30]. The high porosity and large surface area of the nanofiber mat is expected to increase the interaction between the Cur and tissue and also modulate the cellular function to promote the wound-healing process. The morphology of PLA nanofibers containing different amounts of Cur was observed via field emission-scanning electron microscopy (FE-SEM). The miscibility of Cur and PLA in the blended nanofibers was evaluated by attenuated total reflection Fourier transform infrared (ATR-FTIR) spectroscopy and tensile tests. The bioactivity of Cur-loaded PLA nanofiber mats were examined in vitro using C2C12 myoblast cells to assess its cytotoxicity as well as the attachment and proliferation of the cultured cells. In vivo wound-healing assays using PLA and Cur-loaded PLA nanofiber treatments were investigated in a mouse model.

Experimental

Materials

PLA with an average molecular weight of 200,000 g/mol (2002D-Grade) was supplied by NatureWorks Co. (USA). Curcumin was purchased from the Institute of Chemistry, Vietnam. All solvents, including *N,N*-dimethylacetamide (DMAc, 98.5 %) and chloroform (99.0 %), were purchased from Samchun Chemical Co. (Korea). All chemicals were used without further purification.

Fabrication of Cur-loaded PLA nanofibers

A blend of PLA and Cur were dissolved in a mixture of chloroform and DMAc at an 80:20 weight ratio. The PLA concentration was 8 wt% and the amount of Cur was calculated as a weight percentage of PLA to be 0.125, 1.250, and 6.250 wt% for various samples. Each of the prepared solutions was poured into a standard 5-mL plastic syringe that was attached to a blunt 22-gauge stainless steel hypodermic needle. The solution flow rate was controlled using a syringe pump (KD scientific, Model KDS200, USA). An aluminum sheet was wrapped around a rotating collector that was connected to the negative electrode. A high-supply voltage (Chungpa EMI, Korea) was applied to the hypodermic needle as a positive electrode. The polymer solution was electrospun at a positive voltage of 11 kV, a needle tip-to-collector distance of 12 cm and a solution flow rate of 1 mL/h. All the electrospinning processes were carried out at approximately 25 °C and 20 % humidity.

Characterization

The morphology of the electrospun Cur-loaded PLA nanofibers was investigated using field emission-scanning electron microscopy (FE-SEM) (HITACHI S-4700, Japan) with a coating system (MED020, Bal-Tech, USA). The average fiber diameter, distribution, and standard deviation were determined from the FE-SEM photographs using visualization software (TOMORO ScopeEye 3.6).

The chemical characteristics of Cur and Cur-loaded PLA nanofibers were determined via ATR-FTIR analysis (JASCO, ATR-FTIR 6100, Japan).

The mechanical performance of the nanofiber mats was characterized using a tensile tester (LR 5 K, LLOYD instrument, UK) with a load cell of 10 N. The electrospun scaffold of each sample was cut into 50 × 10 mm strips and the dimension of the gauge was 10-mm width by 30-mm length; its thickness was varied between 80 and 100 μm by controlling the electrospinning time. Each tensile test was performed at room temperature with a crosshead speed of 5 mm/min and a preload of 0.1 MPa. All reported tensile strength and tensile stress values represent the average of 6–7 measurements.

Contact angle measurements were carried out in order to determine the surface hydrophobicity of fabricated nanofibers. Immediately after deionized water was allowed to fall freely onto the surfaces of flat non-woven mats, contact angles were measured using a video contact angle instrument (Samsung FA-CED camera, South Korea). The average of five measurements carried out at different locations on the surface of a non-woven mat was considered as the final contact angle value.

In vitro cytotoxic test

Cell seeding on Cur-loaded PLA nanofiber mats

Cur-loaded PLA nanofiber mats (50 μm thick) were cut into circular disks with either ~7 mm or ~15 mm diameters. The disk specimens were placed at the bottom of the wells of 96-well and 24-well culture plates (Nunc, Denmark), respectively. Each sample underwent each treatment in triplicate. Plates containing the core/sheath composite nanofiber mats were sterilized overnight under UV light. A mouse myoblast cell line (i.e., C2C12) was seeded onto the nanofiber mats at a density of 1.5×10^4 cells/mL in the 96-well and 24-well culture plates. The cells were then incubated at 37 °C for 1, 3, and 5 days.

Cell viability assay

Cell viability was determined using a cell counting kit ((CCK)-8, Dojindo Laboratories, Japan) according to the

manufacturer's instructions. Briefly, after each time period (i.e., 1, 3, and 5 days), 10 μL of CCK-8 solution was added to each well of the 96-well plate that contained cells embedded on nanofiber mats. Next, the plate was incubated at 37 °C under 5 % CO₂ for 2 h. Finally, the absorbance at 450 nm was measured using a microplate reader (Infinite F50, Switzerland). Each assay was carried out in triplicate.

Cell attachment to the nanofiber mats

Cell attachment was observed at each time point using SEM. The seeded nanofiber mats in the 24-well plates were washed with PBS and fixed for 30 min at room temperature using a 2.5 wt% glutaraldehyde (Junsei Chemical Co., Japan) PBS solutions. The nanofiber mats were then dehydrated by immersion in a series of ethanol solutions (30, 50, 70, and 90 % v/v). Samples were dried overnight at room temperature, coated with palladium using the MED020 instrument (Bal-Tech system, USA), and then observed using SEM (Hitachi S-3600N, Japan).

Statistical analysis

The statistical analysis of the data was performed using one-way analysis of variance (ANOVA) for statistical significance of three groups ($p < 0.05$). Data points are presented as mean ± standard deviation; the error bars represent the standard deviation.

Wound healing assay

Female C57BL/6 mice (14–16 g) were housed under standard conditions with controlled temperature (23 °C) and a light/dark cycle (12/12 h). The animals were anesthetized with Avertin. To create a wound on the animals, the dorsal hairs of the mice were completely shaved, and then hot circular metal sticks (7 mm in diameter) were brought into contact with the hairless dorsal skin for 2 s. The wound areas were sterilized with povidone iodide. After 1 day, the dead skin around the wound was excised to the full thickness with scissors and tweezers. The wounds were dressed with Cur-loaded PLA nanofiber scaffolds, and then covered with commercial gauze, as shown in Fig. 1. Wounds dressed with only gauze or PLA nanofiber scaffolds were also prepared as controls.

Results and discussion

Morphology of electrospun nanofibers

The morphology of the electrospun PLA nanofibers, Cur-loaded PLA nanofibers, and the diameter distributions are

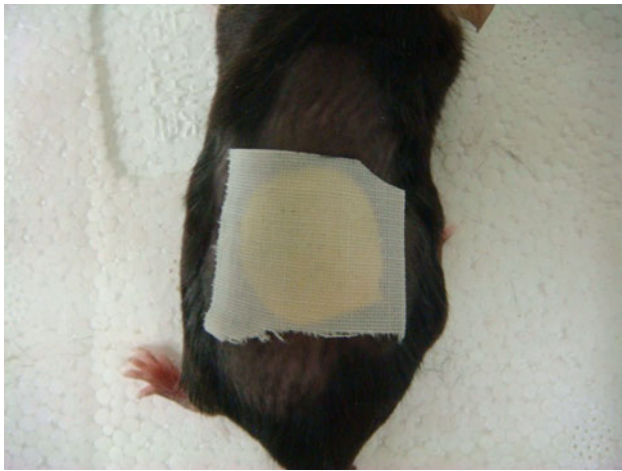


Fig. 1 Treatment of wound area with electrospun Cur-loaded nanofibers

shown in Fig. 2. The average diameters of these fibers are listed in Table 1. The effects of several parameters on the morphology of PLA fibers have been reported by some scientists. Gu and Ren [31] found that the diameter of PLA fibers increases with the increasing polymer concentration and decreases with the increasing applied voltage. Ribeiro et al. [32] reported the effect of solution feed rate and type of collector on diameter and orientation of PLA fibers. The average fiber diameter increases with the increasing solution feed rate and was larger at the lowest rotating speeds with random fiber orientation when using rotating collector. At higher rotation speeds, the fibers had smaller diameter and were aligned in one preferential direction. It was reported that the use of different solvent systems resulted in different nanostructures of electrospun PLA nanofibers [33]. In this study, the PLA nanofibers electrospun from a mixture of chloroform and *N,N*-dimethylacetamide (DMAc) solvents showed a typical nanostructure with largely unconnected single nanofibers. Meanwhile, electrospinning of PLA from the solvent containing THF led to a considerable extent of branching and fiber connectivity [34]. Four key properties of solvent, including dielectric constant, surface tension, conductivity, and volatility, are particularly important effects on electrospinning process and morphology of electrospun materials [33, 35]. In our previous study [36], a mixture of dichloromethane (DCM) and DMAc was used as solvent system for electrospinning of PLA. The results showed that the surface of obtained PLA nanofibers contained irregular pores which were closely spaced. In this case, phase separation caused by the use of mixture consisting of a volatile good solvent (DCM) and a non-volatile poor solvent (DMAc) is thought to be a key step in the formation of pores.

At the same processing conditions (i.e., solvent system, voltage, feed rate, distance from needle tip-to-collector, needle diameter, and collector rotating speed), the PLA nanofibers and Cur-loaded PLA nanofibers with different amounts of Cur had similar morphology without aggregation of Cur particles on the surface. The incorporation of Cur led to a reduced diameter of the electrospun nanofibers and a narrow distribution of the fiber diameter. The mean diameter of the PLA nanofibers was estimated to be 971 nm with a range of 500–2000 nm, while that of Cur-loaded PLA nanofibers containing 6.250 wt% Cur was 562 nm with a range of 300–1200 nm. Therefore, it is evident that increasing the amount of Cur in PLA significantly decreases the diameter of the nanofibers and improves the fiber uniformity. An interconnected porous structure formed by nanofibers lying loosely upon each other was observed. This structure mimics the natural extra cellular matrix (ECM) and provides open space for cell attachment and proliferation. In addition, this porous structure is extremely efficient for hemostasis, fluid absorption, and gas exchange, which ensure a sufficiently moist environment for promoting wound healing and preventing scar formation.

Chemical characterization of the surface of Cur-loaded PLA nanofibers

Chemical characterization of the surface of Cur-loaded PLA nanofibers was performed via ATR-FTIR analysis, as shown in Fig. 3. The ATR-FTIR spectra of PLA nanofibers and Cur-loaded PLA nanofibers with different amounts of Cur show some absorption bands with similar characteristics. The mountainous triplet peak at 1050, 1095, and 1140 cm^{-1} and peak at 1195 cm^{-1} correspond to C–O stretching vibration, while the sharp, intense peak at 1760 cm^{-1} was assigned to C=O stretching. The two peaks at 1395 and 1450 cm^{-1} and the broad band at 2920 cm^{-1} involve to the symmetrical stretching of the CH_3 group. All the above-mentioned absorption bands are characteristic of PLA functional groups and also appear in the ATR-FTIR spectra of the Cur-loaded PLA nanofibers. Additional absorption bands due to the presence of Cur were also observed in the spectra of the Cur-loaded PLA nanofibers. The peaks corresponding to the C=C aromatic stretching frequency of Cur at 820 and 855 cm^{-1} shifted to 760 and 870 cm^{-1} in the spectra of the Cur-loaded PLA nanofibers. The mountainous peaks at 1360–1395 cm^{-1} and 2995 cm^{-1} in the Cur-loaded PLA nanofibers spectra were not observed in the spectra of PLA nanofibers or Cur powder; this indicates that the symmetry of the $-\text{CH}_3$ group in Cur was disrupted upon blending with PLA. The peaks corresponding to the olefin stretching vibrations at 1500 and 1600 cm^{-1} were intense

Fig. 2 Morphology of **a** electrospun PLA nanofibers and **b–d** electrospun Cur-loaded PLA nanofibers with **b** 0.125, **c** 1.250, and **d** 6.250 wt% Cur. The graphs (**a'–d'**) show the distribution of nanofibers diameters in (**a–d**), respectively

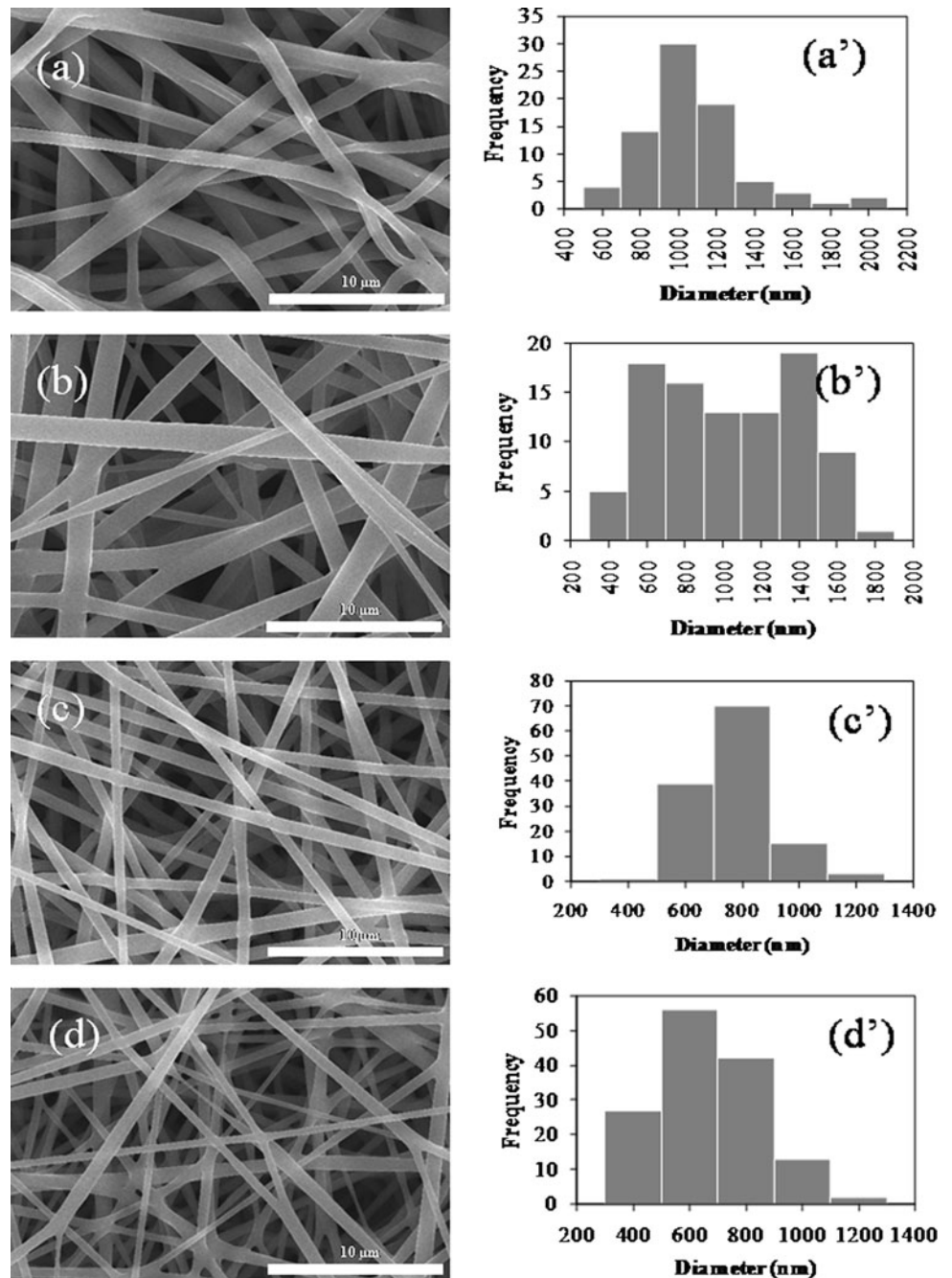


Table 1 Average diameter of electrospun PLA nanofibers and electrospun Cur-loaded PLA nanofibers with different amounts of Cur

Percent of Cur (wt%)	Average diameter (nm)
0	971 ± 274
0.125	943 ± 383
1.250	666 ± 130
6.250	562 ± 177

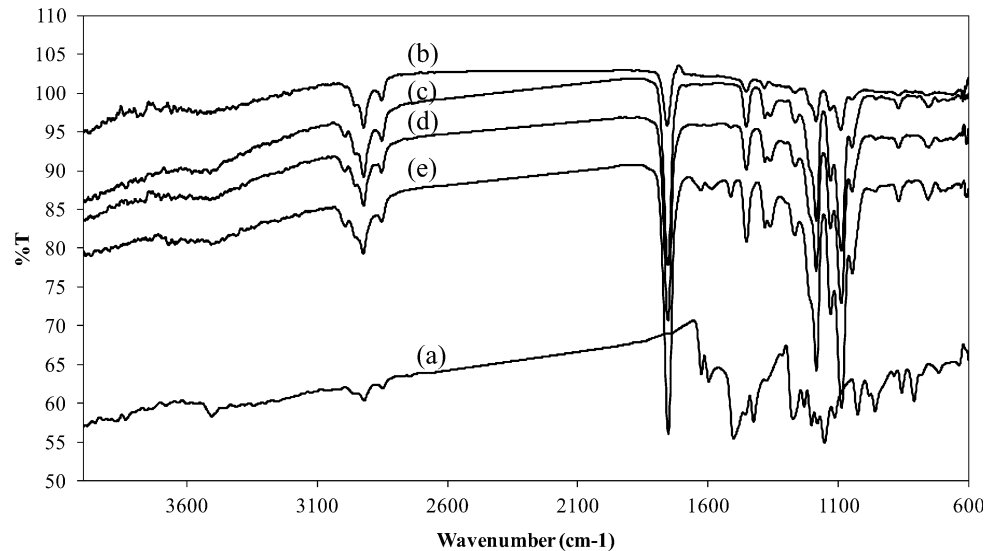
in the spectra of PLA nanofibers containing 6.250 wt% Cur, which might be due to the high content of Cur on the surface of the nanofibers as well as poor miscibility

between Cur and PLA in the blended nanofibers at this concentration of Cur.

Mechanical characterization of Cur-loaded PLA nanofibers

The effect of Cur content in the blends on the mechanical strength of Cur-loaded PLA nanofiber mats was assessed using tensile tests. The stress–strain curves of the electrospun non-woven mats of PLA nanofibers and Cur-loaded PLA nanofibers are shown in Fig. 4. The non-woven mat of

Fig. 3 ATR-FTIR spectra of **a** curcumin, **b** PLA nanofibers, and **c–e** Cur-loaded PLA nanofibers with **c** 0.125, **d** 1.250, and **e** 6.250 Cur



PLA nanofibers had a tensile stress of 2.5 MPa and a tensile strain of 143 %. The incorporation of 0.125 and 1.250 wt% Cur into PLA nanofibers led to a significant increase in the tensile stress (3.5 and 3.5 MPa, respectively). There was a negligible difference in the tensile strength of these samples, which indicates that PLA and Cur showed good miscibility at these ratios. Therefore, both ATR-FTIR analysis and tensile testing revealed strong interactions between Cur and PLA in the blend. The addition of more Cur (6.250 wt%) decreased the elongation and tensile strength of Cur-loaded PLA nanofibers compared with that of PLA nanofibers. This might be attributed to the lower homogeneity of the microstructure of PLA due to excess Cur molecules in the Cur/PLA blend. It is worth noting that the mechanical properties of PLA nanofibers containing <1.250 wt% Cur are sufficient for wound-dressing materials.

In vitro cytotoxic assay

The use of fabricated nanofibers as wound dressings was investigated by cytotoxic testing, which involved the direct culture of C2C12 cells on a PLA nanofiber mat and on Cur-loaded PLA nanofiber mats for 1, 3, and 5 days. The viability of the cells, which correspond to cell survival, was determined using by cell counting kit-8 assay, as shown in Fig. 5. The cells cultured on polystyrene well plates as control samples gradually proliferated during 5 days of cell incubation. The viability of the cells seeded on nanofiber mats was less than 50 % of that of the control sample, which might be due to the hydrophobicity of the PLA nanofiber surface and Cur component (The water contact angle measured on the surface of PLA nanofiber mat and Cur-loaded PLA nanofiber mat were $110^\circ \pm 1.5$ and $113^\circ \pm 1.8$, respectively). There was a negligible difference in cell

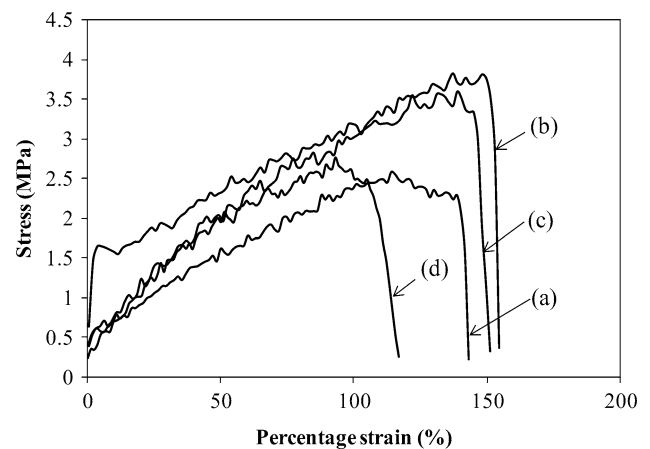


Fig. 4 Mechanical strength of **a** PLA nanofibers and **b–d** Cur-loaded PLA nanofibers with **b** 0.125, **c** 1.250, and **d** 6.250 wt% Cur

viability after 1 and 3 days incubation for the PLA and Cur-loaded PLA nanofibers; however, there was significant cell proliferation between days 3 and 5.

It has been reported that the cytotoxic activity of Cur toward different cells is dependent both on the dose and the type of cell line. In general, Cur exhibits cytotoxic effects at high concentrations of approximately 25 μM . The treatment of Caki cells with 50 μM Cur resulted in the activation of caspase 3, cleavage of phospholipase C- γ 1, and DNA fragmentation [37]. Meanwhile, fibroblast-mediated collagen gel contraction in an in vitro wound contraction model was completely prevented by 25 μM Cur [38]. In this study, the release of Cur from Cur-loaded nanofibers in a cell culture medium was investigated in order to test the effect of Cur concentration on cell growth. PLA nanofibers and Cur-loaded nanofibers were incubated separately on cell culture mediums; and the absorption of

the extraction medium was measured at 1, 3, and 5 days of incubation. The results indicated that no significant difference in absorption of medium and extraction medium was observed during this time. It is suggested that the effect of Cur mainly occurs via contact between cells and Cur on the surface of the nanofibers. The viability of the cultured cells on PLA nanofibers containing 0.125 wt% Cur was higher than that of cells cultured on PLA nanofibers only; this indicates that the inclusion of Cur in PLA nanofibers could induce cell proliferation. However, the viability of cultured cells was found to decrease with the increasing amount of Cur loaded onto the PLA nanofibers. Evidently, a cytotoxic dose of Cur on the surface of the nanofibers was reached above 1.250 wt% Cur.

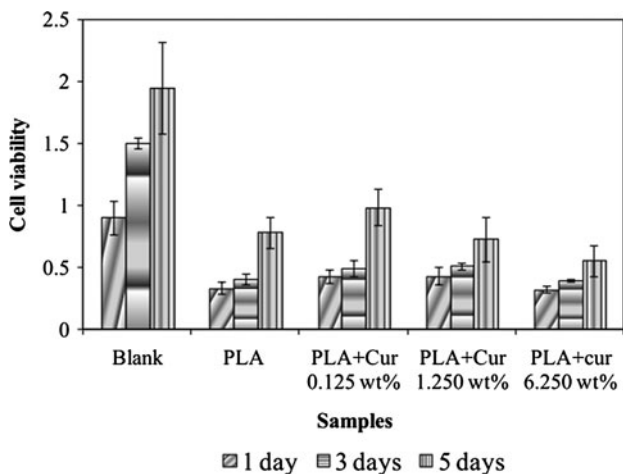


Fig. 5 Cell viability assay of PLA nanofibers and Cur-loaded PLA nanofibers with different amounts of Cur. Values are expressed as mean \pm SD of three parallel measurements. The 1, 3, and 5 days values are compared separately ($p < 0.05$)

Cell attachment on nanofiber mats

Cell attachment on nanofiber mats

The attachment and proliferation of cells cultured on the surface of PLA nanofibers and Cur-loaded PLA nanofibers for 3 days were evaluated by SEM (Fig. 6). It is evident that the cells attached to the nanofiber mats maintained their characteristic spindle-like morphology. The cells firmly adhere to the nanofiber mats and partly enmesh under the nanofiber layer. In agreement with the results obtained from the CCK-8 assay, the number of cells proliferating on the surface of 0.125 wt% Cur-loaded PLA nanofiber mats was greater than that on the surface of the PLA nanofiber mat. The cells readily dispersed both on the surface and under a thin layer of the 0.125 wt% Cur-loaded PLA nanofiber mats during proliferation, which implies good biocompatibility of Cur-loaded PLA nanofibers at this Cur concentration. However, fewer cells were observed on the surface of Cur-loaded PLA nanofibers containing higher Cur concentration, as shown in Fig. 6d; this clearly indicates the adverse effects of Cur on cell behavior at high Cur doses.

Fig. 6 The morphology of C2C12 cell attached to **a** PLA nanofibers and **b–d** Cur-loaded PLA nanofibers with **b** 0.125, **c** 1.250, and **d** 6.250 wt% Cur after 3 days

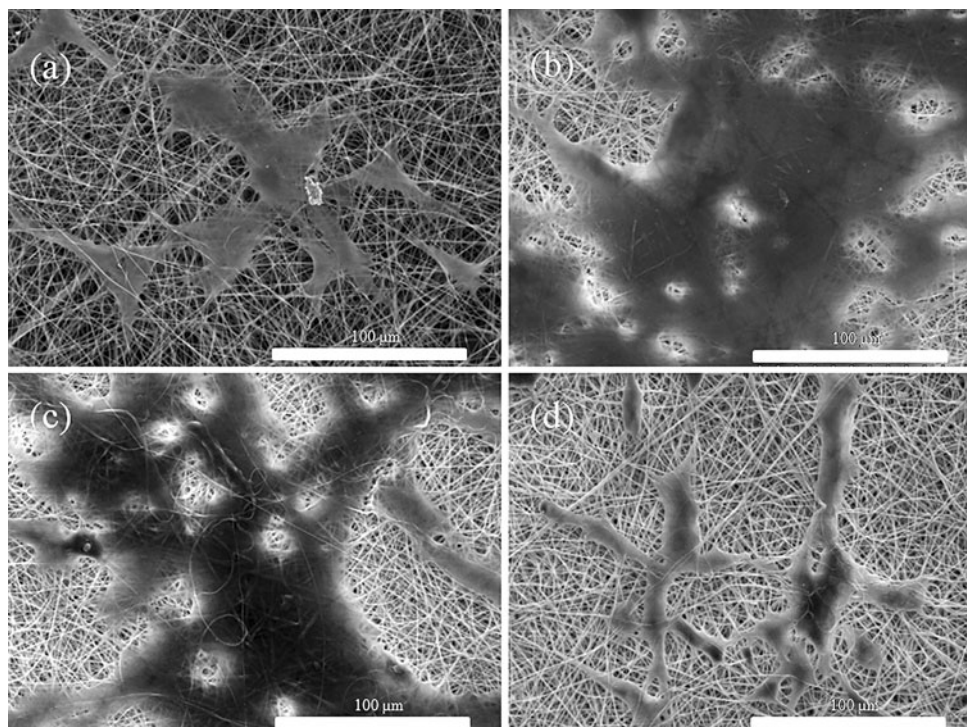


Fig. 7 Photographs of the closure of control, PLA nanofibers-treated, and Cur-loaded PLA nanofiber-treated mouse back wounds on days 0, 7, and 15

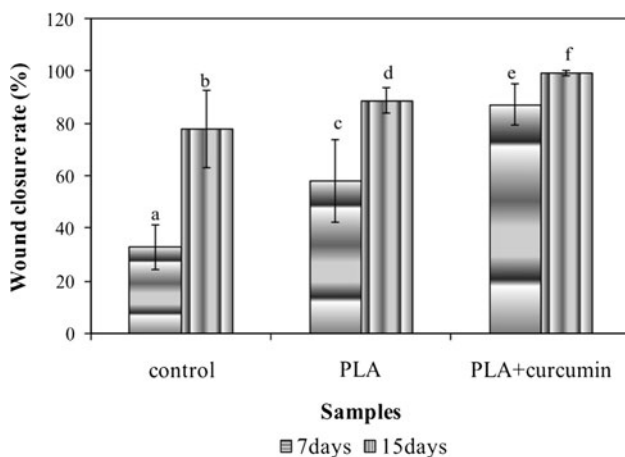
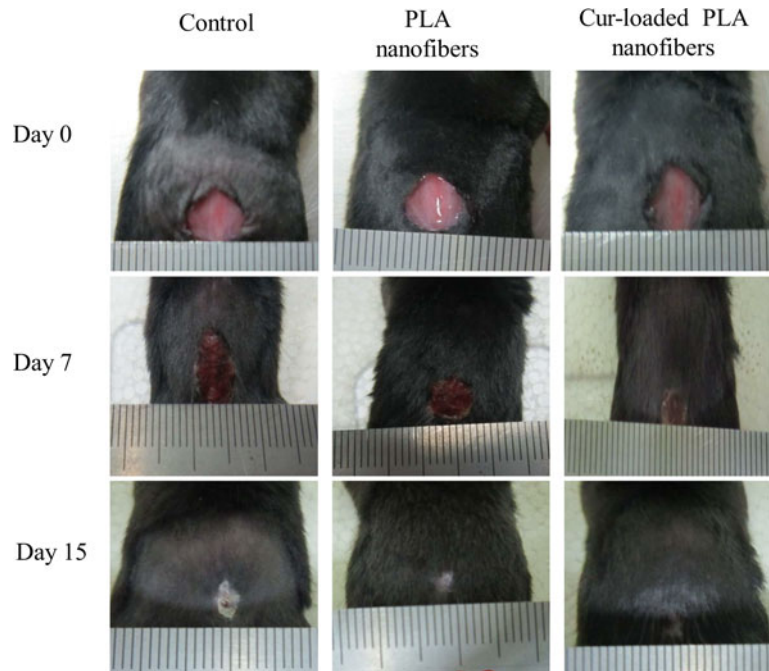


Fig. 8 The rate of wound closure in control and nanofiber mat-treated wounds after 7 and 15 days. Wound closure rate = $(\text{lesion area}_{\text{day}\#} - \text{lesion area}_{\text{day}0}) / \text{lesion area}_{\text{day}0}$; lesion areas were calculated by multiplying a length to a width (cm^2). The average values and standard deviations are presented in the graph ($n = 5$). The wound closure rates of different samples at 7 and 15 days were compared separately. The bars with different letters are significantly different $p < 0.05$

In vivo wound closure assay

Wound healing is a special biological process that comprises four consecutive phases: (1) hemostasis and inflammation, (2) migration, (3) proliferation, and (4) tissue remodeling. It is generally more than 2 weeks between the moment of injury and complete fibroblast coverage of the surface of the wound as a new layer of skin. For years,

people have used different materials such as honey, animal fats, and plant extracts including Cur to encourage the wound-healing process. Modern research had revealed that Cur possesses significant antioxidant activity, which could help to prevent oxidative damage [20]. Moreover, Cur has been shown to accelerate re-epithelialization of the epidermis and enhance the collagen synthesis, which facilitates wound closure. In this study, the wound-healing properties of Cur-loaded PLA nanofibers mats were examined via an in vivo wound-closure assay on the dorsal wounds of mice. The rates of the closure of wounds treated by gauze (as the control), PLA nanofiber mats, and Cur-loaded PLA nanofiber mats are depicted in Figs. 7, 8. Wounds treated with a PLA nanofiber mat showed a significant increase in the rate of wound closure compared with the control: on day 7, the closure rate of wounds treated with PLA nanofiber mats was almost 58 %, while only approximately 33 % wound closure was observed in the control samples. It is worth noting that PLA nanofiber mat without containing any therapeutic compounds promote wound closure. This might be due to the biocompatibility of PLA as well as the porous nature of nanofiber mats. The high surface area to volume ratio and the porous structure of nanofiber mats could maintain an ideal environment at the wound interface via absorption of exudates, gas and fluid exchanges, and bacterial protection.

The wounds treated with Cur-loaded PLA nanofiber mats healed much faster: 87 and 99 % wound closure was observed on days 7 and 15, respectively. From Fig. 7, it is evident that re-epithelialization of the wound treated with Cur-loaded PLA nanofibers was almost complete on day 7,

while this stage took nearly 15 days for the untreated wound. On day 15, a new layer of skin with little scarring was present on wounds treated with Cur-loaded PLA nanofibers. In Cur-treated wound, Panchatcharam et al. [20] reported that there is an increase in the levels of hexosamine and uronic acid, which facilitate greater cell mobility, early remodeling, and promote faster healing without scar formation.

Conclusion

PLA nanofibers loaded with different concentrations of Cur (i.e., 0.125, 1.250, and 6.250 wt%) were fabricated using a solution electrospinning technique. Increasing of Cur loading significantly decreased the diameter of the nanofibers and narrowed the size distribution. Chemical and mechanical characterization of the Cur-loaded PLA nanofibers indicated high miscibility between Cur and PLA at lower than 1.250 wt% Cur. The biological activity of Cur was determined to be highly concentration dependent: 0.125 wt% Cur-loaded PLA nanofibers induced C2C12 cell proliferation while higher Cur loadings showed cytotoxic effects toward the cells. Both PLA nanofibers and Cur-loaded PLA nanofibers successfully enhanced the rate of wound closure in vivo in a mouse model. On day 7, the closure rate of wounds treated with Cur-loaded PLA nanofibers was 87 %, which is significantly higher compared than those treated with gauze and PLA nanofibers (33 and 58 %, respectively). This study suggests the potential of Cur-loaded nanofiber mats as effective wound dressings.

Acknowledgements This project was partially financially supported by the “2011 Overseas Benchmarking Program of Hankyong National University”.

References

- Bhardwaj N, Kundu SC (2010) *Biotechnol Adv* 28:325
- Wang HS, Fu GD, Li XS (2009) *Recent Pat Nanotechnol* 3:21
- Sill TJ, von Recum HA (2008) *Biomaterials* 29:1989
- Liang D, Hsiao BS, Chu B (2007) *Adv Drug Deliv Rev* 59:1392
- Zahedi P, Rezaeian I, Ranaei-Siadat SO, Jafari SH, Supaphol P (2010) *Polym Adv Technol* 21:77
- Chong EJ, Phan Lim IJ, Zhang YZ, Bay BH, Ramakrishna S, Lim CT (2007) *Acta Biomater* 3:321
- Powell HM, Supp DM, Boyce ST (2008) *Biomaterials* 29:834
- Choi JS, Leong KW, Yoo HS (2008) *Biomaterials* 29:587
- Khil MS, Cha DI, Kim HI, Kim IS, Bhattarai N (2003) *J Biomed Mater Res B* 67B:675
- Liu SJ, Kau YC, Chou CY, Chen JK, Wu RC, Yeh WL (2010) *J Membr Sci* 355:53
- Chen ZG, Wang PW, Wei B, Mo XM, Cui FZ (2010) *Acta Biomater* 6:372
- Liu X, Lin T, Fang Z, Yao G, Wang XG (2008) *Adv Sci Technol* 57:125
- Schneider A, Wang XY, Kaplan DL, Garlick JA, Egles C (2009) *Acta Biomater* 5:2570
- Bölgen N, Vargel I, Korkusuz P, Menceloğlu YZ, Pişkin E (2007) *J Biomed Mater Res B* 81B:530
- Chen Y, Lin J, Fei Y, Wang H, Gao W (2010) *Fiber Polym* 11:1128
- Kössler S, Nofziger C, Jakab M, Dossena S, Paulmichl M (2012) *Toxicology* 292:123
- Maheshwari RK, Singh AK, Gaddipati J, Srimal RC (2006) *Life Sci* 78:2081
- Srivastava RM, Singh S, Dubey SK, Misra K, Khar A (2011) *Int Immunopharmacol* 11:331
- Notoya M, Nishimura H, Woo JT, Nagai K, Ishihara Y, Hagiwara H (2006) *Eur J Pharmacol* 534:55
- Panchatcharam M, Miriyala S, Gayathri V, Suguna L (2006) *Mol Cell Biochem* 290:87
- Sidhu GS, Singh AK, Thaloor D, Banaudha KK, Patnaik GK, Srimal RC, Maheshwari RK (1998) *Wound Repair Regen* 6:167
- Gou M, Men K, Shi H, Xiang M, Zhang J, Song J, Long J, Wan Y, Luo F, Zhao X, Qian Z (2011) *Nanoscale* 3:1558
- Wang X, Jiang Y, Wang YW, Huang MT, Ho CT, Huang Q (2008) *Food Chem* 108:419
- Kumar V, Lewis SA, Mutalik S, Shenoy DB, Venkatesh, Udupa N (2002) *Indian J Physiol Pharmacol* 46:209
- Gopinath D, Ahmed MR, Gomathi K, Chitra K, Sehgal PK, Jayakumar R (2004) *Biomaterials* 25:1911
- Ratanajajaroen P, Watthanaphanit A, Tamura H, Tokura S, Rujiravanit R (2012) *Eur Polym J* 48:512
- Merrell JG, McLaughlin SW, Tie L, Laurencin CT, Chen AF, Nair LS (2009) *Clin Exp Pharmacol Physiol* 36:1149
- Suwantong O, Ruktanonchai U, Supaphol P (2010) *J Biomed Mater Res A* 94A:1216
- Foldberg S, Petersen M, Fojan P, Gurevich L, Fink T, Pennisi CP, Zachar V (2012) *Colloid Surf B* 93:92
- Evans RGD, Brandt K, Katz S, Chauvin P, Otto L, Bogle M, Wang B, Meszlenyi RK, Lu L, Mikos AG, Patrick CW Jr (2002) *Biomaterials* 23:841
- Gu SY, Ren J (2005) *Macromol Mater Eng* 290:1097
- Ribeiro C, Sencadas V, Costa CM, Ribelles JL, Lanceros-Mendez S (2011) *Sci Technol Adv Mater* 12:015001
- Rahman NA, Gizdavic-Nikolaidis M, Ray S, Easteal AJ, Travas-Sejdic J (2010) *Synth Met* 160:2015
- Gizdavic-Nikolaidis M, Ray S, Bennett J, Swift S, Bowmaker G, Easteal A (2011) *J Polym Sci Polym Chem* 49:4902
- Andrady AL (2008) *Science and technology of polymer nanofibers*. Wiley, New Jersey
- Nguyen TTT, Ghosh C, Hwang SG, Chanunpanich N, Park JS (2012) *Int J Pharm* 439:296
- Woo JH, Kim YH, Choi YJ, Kim DG, Lee KS, Bae JH, Min DS, Chang JS, Jeong YJ, Lee YH, Park JW, Kwon TK (2003) *Carcinogenesis* 24:1199
- Scharstuhl A, Mutsaers HAM, Pennings SWC, Szarek WA, Russel FGM, Wagener FDA (2009) *J Cell Mol Med* 13:712